Neurobiology of Disease

Thalidomide and Lenalidomide Extend Survival in a Transgenic Mouse Model of Amyotrophic Lateral Sclerosis

Mahmoud Kiaei,[1] Susanne Petri,[1] Khatuna Kipiani,[1] Gabrielle Gardian,[1] Dong-Kug Choi,[2] Junyu Chen,[1] Noel Y. Calingasan,[1] Peter Schafer,[3] George W. Muller,[3] Charles Stewart,[4] Kenneth Hensley,[4] and M. Flint Beal[1]

[1]Department of Neurology and Neuroscience, Weill Medical College of Cornell University, New York-Presbyterian Hospital, New York, New York 10021, [2]Department of Biotechnology, Konkuk University, 380-701, South Korea, [3]Celgene Corporation, Summit, New Jersey 07901, and [4]Oklahoma Medical Research Foundation, Oklahoma City, Oklahoma 73104

Accumulating evidence suggests that inflammation plays a major role in the pathogenesis of motor neuron death in amyotrophic lateral sclerosis (ALS). Important mediators of inflammation such as the cytokine tumor necrosis factor-α (TNF-α) and its superfamily member fibroblast-associated cell-surface ligand (FasL) have been implicated in apoptosis. We found increased TNF-α and FasL immunoreactivity in lumbar spinal cord sections of ALS patients and G93A transgenic mice. Both increased TNF-α and FasL immunostaining in the lumbar spinal cord of the G93A SOD1 transgenic mice occurred at 40 – 60 d, well before the onset of symptoms and loss of motor neurons. We tested the neuroprotective effect of thalidomide and its analog lenalidomide, pharmacological agents that inhibit the expression of TNF-α and other cytokines by destabilizing their mRNA. Treatment with either thalidomide or lenalidomide attenuated weight loss, enhanced motor performance, decreased motor neuron cell death, and significantly increased the life span in G93A transgenic mice. Treated G93A mice showed a reduction in TNF-α and FasL immunoreactivity as well as their mRNA in the lumbar spinal cord. Both compounds also reduced interleukin (IL)-12p40, IL-1α, and IL-1β and increased IL-RA and TGF-β1 mRNA. Therefore, both thalidomide and lenalidomide bear promise as therapeutic interventions for the treatment of ALS.

Key words: **G93A; SOD1; thalidomide; lenalidomide; TNF-α; FasL**

Introduction

Amyotrophic lateral sclerosis (ALS) is a fatal disease characterized by an age-related progressive degeneration of both upper and lower motor neurons (Leigh and Ray-Chaudhuri, 1994). Approximately 5–10% of ALS cases are familial and exhibit an autosomal-dominant pattern of inheritance (Siddique et al., 1996). A major discovery in the study of ALS was the finding of missense mutations in the enzyme copper–zinc superoxide dismutase (SOD1), which is associated with 15–20% of familial ALS cases (Rosen et al., 1993). This led to the development of transgenic mouse models and spurred investigations into disease pathogenesis (Gurney et al., 1994; Ripps et al., 1995; Wong et al., 1995; Bruijn et al., 1997). Neuroinflammation is one of the pathological hallmarks in ALS transgenic mice (West et al., 1991; Almer et al., 2001; Ghezzi and Mennini, 2001; Consilvio et al., 2004; Kiaei et al., 2005b).

Tumor necrosis factor-α (TNF-α) is a major inflammatory cytokine that elicits a wide range of biological responses, including neuronal apoptosis (Tewari and Dixit, 1996; Munoz-Fernandez and Fresno, 1998; Venters et al., 2000). TNF-α mediates its biological effects through activation of two distinct receptors, TNF-R1 and TNF-R2 (Tartaglia and Goeddel, 1992). Both TNF-α and its proapoptotic receptor TNF-R1 mRNA are elevated at late presymptomatic stages of disease in the lumbar spinal cord of G93A mice (Hensley et al., 2002, 2003; Yoshihara et al., 2002). Expression of both the cytokine and its receptors continues to increase during the paralytic phase of disease (Hensley et al., 2002, 2003; Yoshihara et al., 2002). Upregulation of TNF-α precedes transcriptional upregulation of other pro-inflammatory gene products and temporally correlates with progression of the disease in G93A mice (Hensley et al., 2002, 2003). A similar elevation of pro-inflammatory cytokines has been reported in slowly progressing strains of G93A SOD1 transgenic mice and in G37R SOD1 mice (Elliott, 2001; Nguyen et al., 2001; Kriz et al., 2002). In addition, both TNF-α and soluble TNF receptor are elevated in serum of humans with ALS (Poloni et al., 2000). TNF-α is capable of activating microglia and causing neurotoxicity in motor neurons that are compromised by accumulation of aggregated proteins (Robertson et al., 2001).

Fibroblast-associated cell-surface ligand (FasL) may play a critical role in the death of motor neurons associated with mutant SOD1 (Raoul et al., 2002). Furthermore, TNF-α can induce FasL (Pinkoski et al., 2002). When TNF-α binds to its receptor (e.g., TNF-R1) similar to the events that take place when FasL binds to Fas, then death-inducing signaling complex (DISC) will form, and caspase-8 is activated, which leads to apoptotic cell death.

Received Sept. 19, 2005; accepted Jan. 15, 2006.

This work was supported in part by grants from the Muscular Dystrophy Association, the Amyotrophic Lateral Sclerosis Association, and the National Institutes of Health (M.F.B., M.K., and Grant NS044154 to K.H.). Thalidomide and lenalidomide were kindly provided by Celgene. We thank Dr. A. Hays for providing human ALS spinal cord samples.

Correspondence should be addressed to Dr. Mahmoud Kiaei, Department of Neurology and Neuroscience, Weill Medical College of Cornell University, 525 East 68th Street, New York, NY 10021. E-mail: mak2026@med.cornell.edu.

DOI:10.1523/JNEUROSCI.5253-05.2006

 0270-6474/06/262467-07$15.00/0

In the present study, we examined the temporal pattern of TNF-α and FasL immunoreactivity in the lumbar spinal cord of G93A mice. Because previous work showed that the proinflammatroy cytokines TNF-α and FasL are elevated in both human and mouse models of ALS, and play a role in the pathogenesis of ALS, we tested the neuroprotective effects of thalidomide and lenalidomide, two immunomodulatory agents that inhibit TNF-α production (Corral et al., 1999; Bartlett et al., 2004).

Materials and Methods

Mice. G93A SOD1 transgenic familial ALS mice (high copy number) (Gurney et al., 1994) were obtained from The Jackson Laboratory (Bar Harbor, ME). All protocols were conducted within National Institutes of Health guidelines for animal research and were approved by the Institutional Animal Care and Use Committee. We maintained the transgenic G93A hemizygotes by mating transgenic males with B6SJLF1/J hybrid females. Transgenic offspring were genotyped by PCR assay of DNA obtained from tail tissue. G93A transgenic mice were assigned randomly to the control (vehicle), 50 mg/kg/d thalidomide, and 100 mg/kg/d thalidomide groups given in 1× PBS suspension by gavage daily. The dosing regimen was partly based on the study by Boireau et al. (1997), in which thalidomide treatment was examined against 1-methyl-4-phenyl-1,2,3,6-tetrahydropyridine toxicity in mice at doses of 25 and 50 mg/kg. We used our starting dose of 50 mg/kg and used 100 mg/kg to examine the effect of a higher dose. Six N1029 (wild-type SOD1 transgenic) mice and six mice from the thalidomide- and vehicle-treated groups were killed at 110 d of age for histological evaluation. For the lenalidomide experiment, G93A mice were assigned randomly to the control (vehicle) and 100 mg/kg/d lenalidomide groups. The lenalidomide dose was based on thalidomide best dose effect in G93A mice. Treatments started from 30 d of age in all cases. Lenalidomide feed admix was blended at Dyets (Bethlehem, PA). Six mice per group were used for neuronal cell counts and immunohistochemistry. Six G93A mice were used from each group at 110 d of age for biochemical analysis. Because of species-specific potency, doses used in this study cannot be extrapolated for human and should be used as guidelines only. The effective and safe dose of thalidomide or lenalidomide for humans remains to be determined in clinical trials.

Survival. The initial sign of disease in G93A transgenic mice is a resting tremor that progresses to gait impairment, asymmetrical or symmetrical paralysis of the hindlimbs, followed by complete paralysis at the end stage. Mice were killed when they were unable to roll over within 20 s after being pushed on their side, and this time point was recorded as the time of death.

Motor function testing (rotarod). Motor function of these mice was assessed by rotarod twice per week starting at 70 d of age. Mice were trained for 2–3 d to become acquainted with the rotarod apparatus (Columbus Instruments, Columbus, OH). The testing began by placing the mice on a rod rotating at 12 rpm, and the time that mice stayed on the rod (until falling off or staying the maximum 5 min) was recorded as a measurement of the competence of their motor function. To determine the onset of symptoms, a 15 rpm for 10 min protocol was used. Three trials were performed, and the best result of the three trials was recorded.

Reverse transcription-PCR. Total RNA (2.5 μg) from spinal cords of G93A mice treated with thalidomide or vehicle and B6SJL controls was transcribed into cDNA using the Superscript First-Strand synthesis system for reverse transcription (RT)-PCR (Invitrogen, San Diego, CA) following the manufacturer's directions.

Real-time quantitative RT-PCR. Real-time quantitative RT-PCR analyses were performed using the Roche (Welwyn Garden City, UK) LightCycler System. The primers used were as follows: TNF-α, sense 5′-GACCCAGTGTGGGAAG-3′ and antisense 5′-GGTTCAGTGATGTAGCGA-3′; glyceraldehyde-3-phosphate dehydrogenase (GAPDH), sense 5′-CCATGGAGAAGGCTGGG-3′ and antisense 5′-CAAAAGTTGTCATGGATGACC-3′.

PCR was performed with the SYBR Green Quantitative RT-PCR kit (Sigma, St. Louis, MO) using 2 μl of diluted cDNA in 20 μl final reaction mixture according to the manufacture's protocol. PCR cycling parameters in the LightCycler were as follows: 95°C for 2 min for one cycle, followed by 95°C for 30 s, 55°C for 30 s, and 72°C for 45 s on single acquisition mode for 40 cycles. After amplification, a melting-curve analysis was performed, and the specificity of the PCR products was confirmed by gel electrophoresis. Template cDNA was replaced with PCR-grade water as a negative control. Calculations of threshold cycle and difference were analyzed with LightCycler analysis software (Roche). The amounts of TNF-α and GAPDH cDNA were calculated using linear regression analysis from standard curves for both TNF-α and GAPDH, and the amount of TNF-α cDNA was expressed as a percentage of GAPDH.

Histological evaluation and stereological analysis. Mice were perfused transcardially with 0.1 M cold PBS for 1 min, followed by cold 4% paraformaldehyde in PBS for 10 min. The spinal cords were dissected carefully, and the lumbar segment was identified using the ribs and the vertebrae as a guide. Tissues were postfixed in 4% paraformaldehyde for 6 h. Blocks were cryoprotected in 30% sucrose for 24 h.

For stereological analysis, serial coronal sections (50 μm thick) were cut through the lumbar (L1–L4) spinal cord enlargements from wild-type controls and vehicle-, thalidomide-, or lenalidomide-treated G93A mice as described previously (Kiaei et al., 2005a). Briefly, cell counts were made within an area demarcated by a horizontal line drawn through the central canal and encompassing the ventral horn of gray matter to include layers 7–9. The size of the *x*–*y* sampling grid was 200 μm. The counting frame thickness was 14 μm, and the counting frame area was 4900 μm^2. Data were expressed as mean ± SEM.

A separate set of sections was collected as free-floating sections and processed for immunohistochemistry. The sections were immunostained with antibodies to TNF-α (Serotec, Raleigh, NC), FasL (Santa Cruz Biotechnology, Santa Cruz, CA), CD40 (Serotec, Oxford, UK), and glial fibrillary acid protein (GFAP; Dako, Carpinteria, CA), using a modified avidin–biotin peroxidase technique. The immunoreaction was visualized using 3,3′-diaminobenzidine tetrahydrochloride dihydrate with nickel intensification (Vector Laboratories, Burlingame, CA) as the chromogen. The sections were mounted onto gelatin-coated slides, dehydrated, cleared in xylene, and coverslipped. The specificity of immunostaining was confirmed by omission of the primary antibody.

Double immunofluorescence was performed to demonstrate the glial localization of TNF-α and FasL. Sections were incubated for 18 h in the primary antibody mixture containing anti-TNF-α or anti-FasL and the astrocyte marker anti-GFAP. After rinsing with PBS, sections were incubated for 1 h in a mixture of Cy2-conjugated anti-rabbit IgG and Cy3-conjugated anti-mouse IgG (both at 1:200 in 0.5% BSA/PBS).

Human tissues. Paraffin-embedded spinal cord tissues from ALS patients ($n = 6$; four males and two females) and non-neurological disease controls ($n = 6$; three males and three females) were kindly provided by Dr. A. P. Hays (Columbia Presbyterian Medical Center, New York, NY). One of the ALS patients had an I113T mutation of the *SOD1* gene. Controls consisted of patients diagnosed with one of the following: cardiac disease, human immunodeficiency virus/peritoneal hemorrhage, diabetes/cardiac disease, chronic lymphocytic leukemia/sepsis, or cardiac failure. The mean age at death was 59 years (range, 27–69) for ALS patients and 65 years (range, 54–73) for controls.

Paraffin sections (7 μm thick) were prepared and processed for TNF-α or FasL immunohistochemistry as described above. Before immunostaining, the sections were incubated in an antigen unmasking solution (pH adjusted to 3.0; Vector Laboratories) at 37°C for 30 min.

Multiprobe ribonuclease protection assays. Total RNA was extracted from rapidly frozen spinal cord (one-half cord from each mouse) using a method described previously (Hall et al., 1998). Commercial ribonuclease protection assay (RPA) probe sets (PharMingen, San Diego, CA) were used to detect specific RNAs. Radiolabeled probes were synthesized from DNA templates containing a T7 RNA polymerase promoter. Radiolabeled probes were mixed and hybridized with 5–10 μg of total RNA and treated with RNase A and T1 and resolved on 5% polyacrylamide/8 M urea gels. Dried gels were developed using a PhosphorImager (Storm 840 PhosphorImager; Molecular Dynamics, Sunnyvale, CA), and bands were quantified using instrument-resident software.

Statistical analysis. Kaplan–Meier survival analysis and Logrank (Mantel–Cox) were used for survival comparisons. ANOVA was followed by

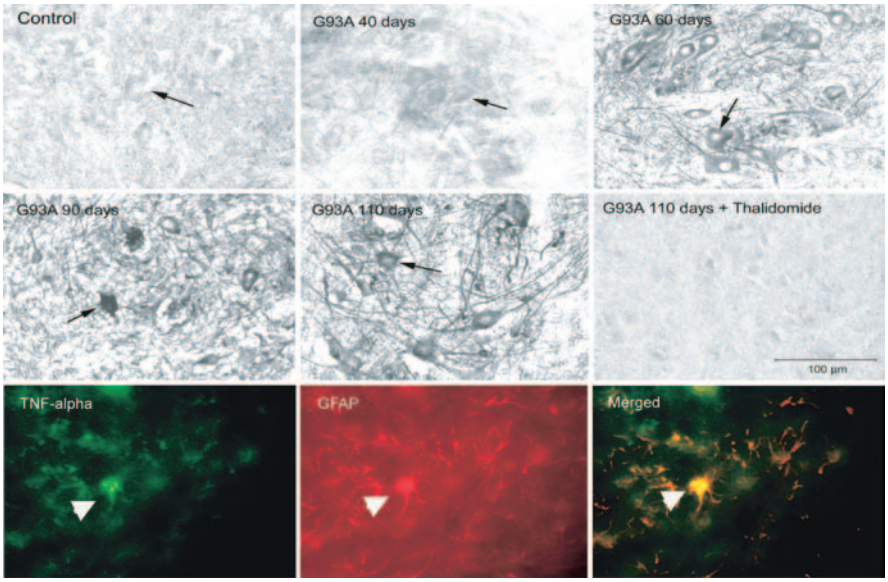

Figure 1. TNF-α immunoreactivity in G93A SOD1 and control mice. TNF-α immunoreactivity was examined in the spinal cords of transgenic G93A SOD1 mice at 40, 60, 90, and 110 d of age and in 110-d-old transgenic wild-type hSOD1 (N1029) control mice. TNF-α immunoreactivity is seen in the anterior horn motor neurons (arrows), with heavy staining in the cytoplasm and nucleus of motor neurons. Thalidomide treatment reduced TNF-α immunoreactivity (middle row, left panel). TNF-α double immunofluorescence with GFAP showed that TNF-α colocalizes with GFAP in astrocytes. The white arrowhead points to an astrocyte labeled with TNF-α (green) and GFAP (red) and colocalization of TNF-α and GFAP (yellow). Scale bars: top and middle panels, 100 μm; bottom panels, 66 μm.

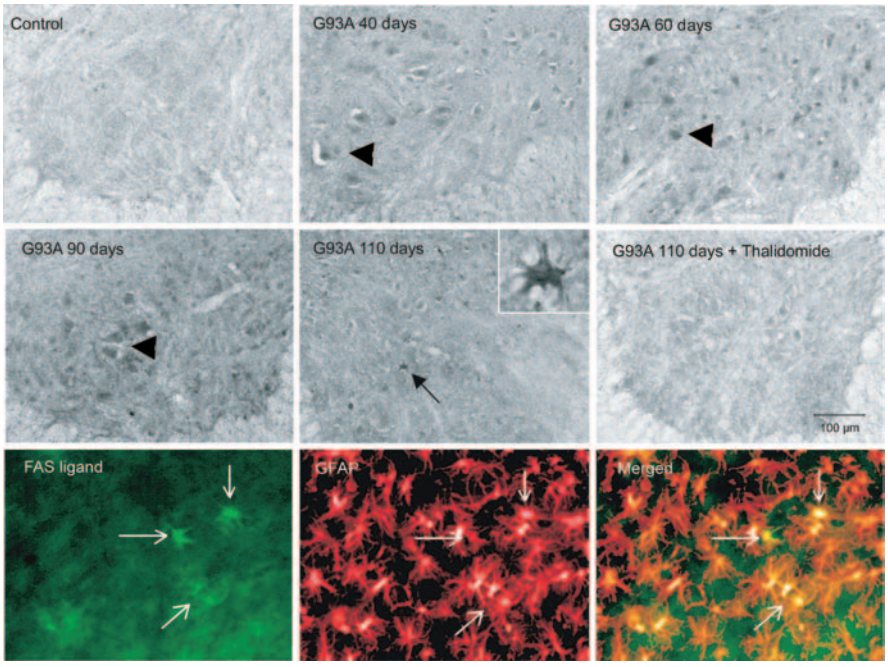

Figure 2. FasL immunoreactivity in G93A SOD1 and control mice. FasL immunoreactivity in neurons of the ventral horn of the lumbar spinal cord in control (N1029; 110 d) and G93A mice killed at 40, 60, 90, and 110 d shows varying levels of immunoreactivity. Increases in FasL staining in neurons (arrowheads) and neuronal processes occurred as early as 60 d in G93A mice. The arrow points to an intensely stained astrocyte; a higher-magnification image is shown in the inset. Thalidomide treatment reduced FasL immunoreactivity (middle row, left panel). FasL double immunofluorescence with GFAP showed that FasL colocalizes with GFAP in astrocytes. The white arrows point to astrocytes labeled with FasL (green) and GFAP (red) and colocalization of FasL and GFAP (yellow). Scale bars: top and middle panels, 100 μm; bottom panels, 33 μm.

the Newman–Keuls test to determine statistical differences in lumbar spinal cord neuron counts between groups. Repeated-measures ANOVA was used for rotarod comparisons. The Mann–Whitney test was used for real-time PCR data.

Results

TNF-α and FasL immunoreactivity in G93A SOD1 mouse model of ALS

We investigated the temporal pattern of TNF-α and FasL immunoreactivity in G93A SOD1 mice at 40 and 60 d (asymptomatic), 90 d (early symptomatic), 110 d (fully symptomatic), and end stage (120–135 d) in the ventral horn of the lumbar spinal cords. Immunohistochemical analysis showed little TNF-α immunoreactivity at 40 d, which appeared similar to controls in the motor neurons of the ventral horn in the lumbar spinal cord. At 60 d, motor neurons from G93A mice with a healthy appearance were stained with TNF-α moderately, and immunoreactivity became more intense at 90 and 110 d. The remaining atrophied motor neurons were less intensely stained at end stage (Fig. 1). TNF-α colocalized with the motor neuron marker (SMI-32) (Kiaei et al., 2006) in the lumbar spinal cord section of G93A mice. TNF-α staining also occurred in actrocytes at 110 d of age as demonstrated by colocalization with the astrocyte marker GFAP by double immunofluorescence (Fig. 1).

Strong immunoreactivity for FasL was evident in neurons as early as 40 d. However, FasL immunoreactivity was less pronounced at 110 d (Fig. 2). Both TNF-α and FasL immunoreactivity persisted relatively strong in the lumbar spinal cord sections of G93A mice at end stage (data not shown). We also examined the FasL immunoreactivity in astrocytes by double labeling with the astrocyte marker GFAP. FasL immunoreactivity colocalized with GFAP, indicating that FasL immunostaining was found in both neurons and astrocytes similar to TNF-α.

TNF-α and FasL immunoreactivity in human ALS

Consistent with the immunohistochemical findings in ALS transgenic mice, intense TNF-α and FasL immunoreactivity occurred in the lumbar spinal cord sections from an ALS patient with a SOD1 mutation (I113T) as well as sporadic ALS patients, whereas control tissues showed very little or no TNF-α and FasL immunoreactivity (Fig. 3). TNF-α and FasL coexisted in the motor neurons.

Thalidomide and lenalidomide treatment

We investigated the effect of thalidomide and lenalidomide treatment in G93A mice. Oral administration of thalidomide resulted in a significant improvement in the survival of G93A mice in a dose-dependent manner compared with the survival of G93A mice treated with saline (see Fig. 5). After oral administra-

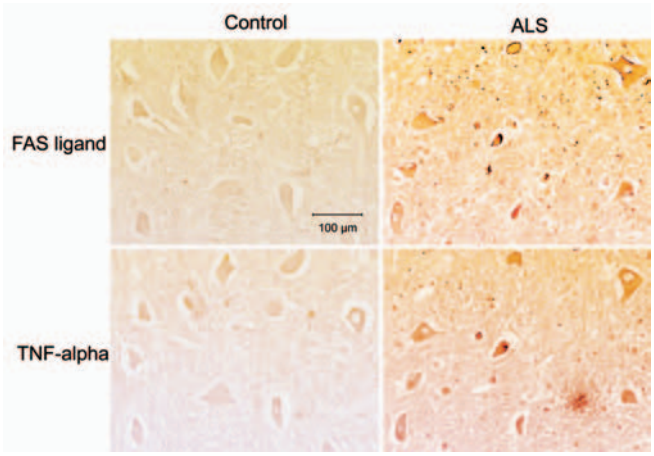

Figure 3. TNF-α and FasL immunoreactivity in human ALS and controls. FasL (top panels) and TNF-α (bottom panels) immunoreactivities in the lumbar ventral horn of the spinal cord of human ALS and control patients. We found TNF-α- and FasL-immunoreactive neurons in the lumbar spinal cord sections of a familial ALS patient with SOD1 mutation (I113T) and sporadic ALS patients. Intense TNF-α and FasL immunoreactivity occurred predominantly in neurons of ALS patients. Coexistence of TNF-α and FasL occurred in the same neurons in adjacent sections of ALS patients. Scale bar, 100 μm.

tion of lenalidomide in mice, it rapidly absorbed into the system circulation with a T_{max} of 42 min for doses of 50 and 200 mg/kg when tested in wild-type mice (data not shown). Lenalidomide treatment in G93A mice resulted in slightly better survival; however, it was not significantly different from thalidomide at 100 mg/kg (see Fig. 5). Each treatment was compared with its own control group. Disease onset was delayed, and the disease progression was slowed with both of the compounds. Histological analysis revealed that the increase in survival was associated with a marked dose-dependent decrease in TNF-α immunoreactivity in the motor neurons and glial cells in the spinal cord lumbar regions of G93A mice compared with saline-treated controls (data not shown). We show that thalidomide treatment reduced TNF-α and FasL immunoreactivity in the spinal cords of G93A mice (Figs. 1, 2).

Motor performance and weight loss

G93A mice treated with thalidomide or lenalidomide had significantly better motor performance from 98 to 155 d of age than mice given saline (Fig. 4). Additionally, thalidomide and lenalidomide attenuated weight loss from the age of 70 d compared with saline-treated G93A controls (data not shown).

Survival

The mean survival in G93A mice treated with 50 mg/kg thalidomide was increased from 130 ± 8.5 d (n = 10) to145 ± 19 d (~12%; n = 10; $p < 0.03$) and with 100 mg/kg thalidomide was increased to 151 ± 19 d (~16%; n = 12; $p < 0.003$) compared with G93A controls treated with saline (Fig. 4). Lenalidomide treatment at 100 mg/kg significantly increased the mean survival of G93A mice from 130 ± 4 d (n = 7) to 154 ± 16 d (n = 12; ~18.5%; $p < 0.0001$) (Fig. 5).

Nissl-stained neuronal cell count

Thalidomide and its analog significantly attenuated neuronal loss in the lumbar spinal cord of G93A mice. The number of surviving Nissl-stained neurons at 110 d of age was significantly higher in G93A mice treated with thalidomide or lenalidomide compared with G93A mice on the control diet ($p < 0.01$) (Fig. 6).

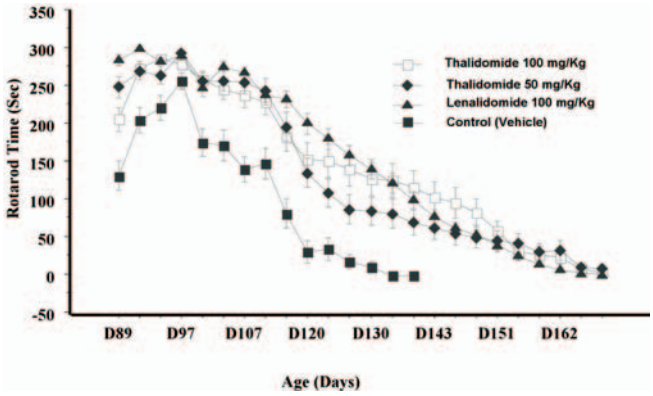

Figure 4. The effect of thalidomide or lenalidomide treatment on motor performance in G93A SOD1 transgenic mice from 89 to 165 d of age. There was significantly improved motor performance in G93A mice treated with both doses of thalidomide ($p < 0.001$) and lenalidomide (100 mg/kg; $p < 0.001$) by repeated-measures ANOVA, followed by Student–Newman–Keuls tests. Values are mean ± SEM. ◆, 50 mg/kg thalidomide; □, 100 mg/kg thalidomide; ▲, 100 mg/kg lenalidomide; ■, vehicle-treated G93A SOD1.

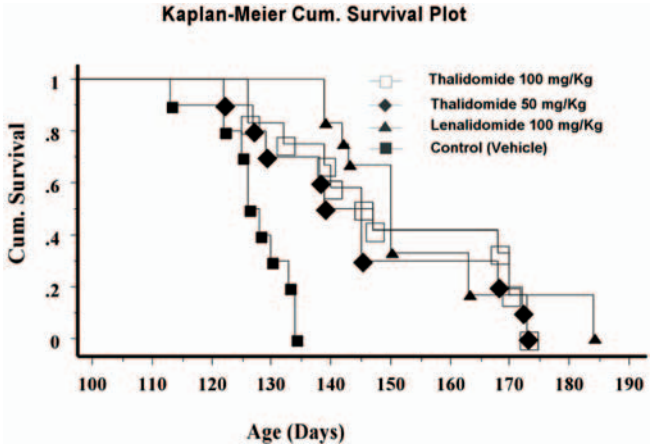

Figure 5. The effect of thalidomide and lenalidomide treatments on survival in G93A transgenic mice. The cumulative (Cum.) probability of survival for mice beginning at 30 d of age treated with vehicle, 50 mg/kg thalidomide, 100 mg/kg thalidomide, and 100 mg/kg lenalidomide is shown. There is a significant increase in survival in treated G93A mice ($p < 0.02$). Values are mean ± SEM. ◆, 50 mg/kg thalidomide; ▲, 100 mg/kg thalidomide; ■, 100 mg/kg lenalidomide; ■, vehicle-treated G93A SOD1.

TNF-α mRNA in G93A mice

To determine whether TNF-α mRNA is upregulated and whether thalidomide and lenalidomide can block its mRNA elevation in the spinal cord of G93A mice, real-time quantitative PCR was performed using cDNA synthesized from total RNA extracted from the spinal cords of G93A SOD1 mice treated with thalidomide or lenalidomide, vehicle-treated G93A mice, and N1029 mice (wild-type SOD1 overexpressers) at 110 d of age. TNF-α mRNA was increased 10-fold in G93A SOD1 mice compared with control littermates ($p < 0.005$) (Fig. 7). Thalidomide and lenalidomide treatment reduced TNF-α mRNA significantly ($p < 0.01$).

Cytokine levels by multiprobe RPAs

Total RNA isolated from the half spinal cords of treated and control G93A mice at 110 d of age were subjected to RPA. RPA showed that both thalidomide and lenalidomide downregulated interleukin (IL)-12p40 and upregulated TGF-β1 and IL-1RA in treated G93A mice compared with vehicle-treated G93A mice (Fig. 8). Lenalidomide also downregulated IL-1α and IL-1β. No

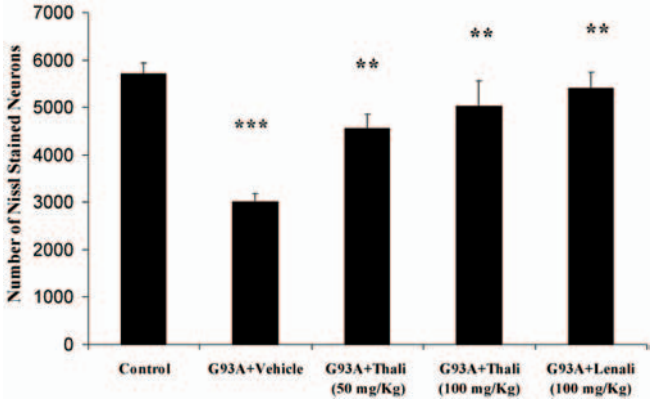

Figure 6. The effect of thalidomide (Thali) or lenalidomide (Lenali) treatment on Nissl-stained neuronal cell counts in G93A SOD1 transgenic mice at 110 d of age. The number of neurons counted by Nissl staining is significantly lower in vehicle-treated G93A mice versus control mice (***$p < 0.001$). Nissl-stained neurons are significantly higher in G93A mice treated with both doses of thalidomide compared with vehicle-treated G93A transgenic mice at 110 d of age (**$p < 0.01$). Nissl-stained neurons are significantly higher in G93A mice treated with lenalidomide compared with vehicle-treated G93A transgenic mice at 110 d of age (**$p < 0.01$) by ANOVA and Student–Newman–Keuls tests. Values are mean ± SEM.

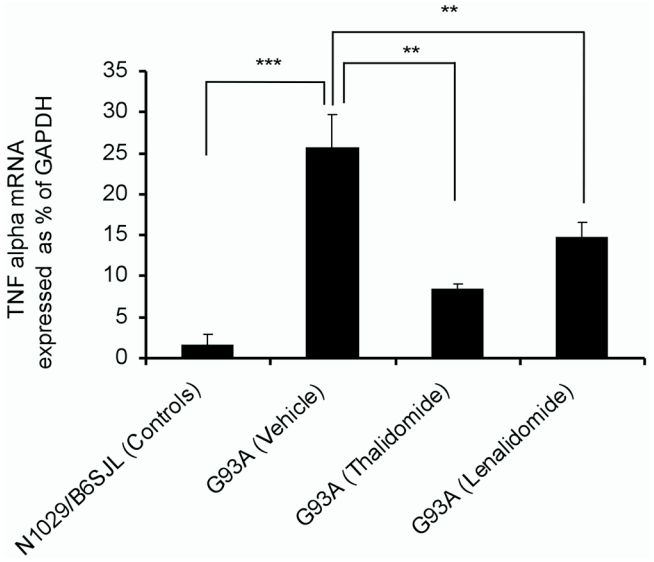

Figure 7. Real-time RT-PCR for TNF-α expression in the spinal cord tissue of G93A SOD1 control mice and G93A mice treated with thalidomide or lenalidomide. The amount of TNF-α cDNA was measured in the total cDNA made from total mRNA isolated from spinal cord tissue of 110-d-old N1029/B6SJL controls and G93A SOD1 mice treated with vehicle, thalidomide, or lenalidomide. TNF-α cDNA amount in different samples was normalized against GAPDH cDNA and expressed as a percentage of GAPDH cDNA (**$p < 0.01$; ***$p < 0.0005$; Mann–Whitney test). There were no changes in GAPDH cDNA amount among the groups. Values are mean ± SEM, representative of three independent real-time PCRs ($n = 5$).

changes were detected in IL-12p35, IL-10, IL-18, IFNγ or IFNβ, IL-6, TGF-β3, and LTα or LTβ (data not shown).

Discussion

Pro-inflammatory cytokines are implicated in ALS pathogenesis. Previous evidence for inflammatory mechanisms in ALS comes from a number of studies (Almer et al., 2001; Elliott, 2001; Hensley et al., 2002; Yoshihara et al., 2002). The loss of motor neurons in transgenic mouse models and in human postmortem tissue is accompanied by a robust glial reaction and microglial activation (Hirano, 1996; Schiffer et al., 1996; Hall et al., 1998). Furthermore, inducible nitric oxide synthase is upregulated in activated microglia in the spinal cord of transgenic ALS mice (Almer et al., 1999). The proinflammatory factors IL-6 and IL-1β are increased in the CSF and spinal cord, respectively, in ALS patients (Almer et al., 1999). IL-1β is also increased in transgenic mouse models of ALS (Ghezzi et al., 1998; Li et al., 2000; Elliott, 2001). Inhibition of IL-1β activation slowed disease progression in a transgenic mouse model of ALS (Li et al., 2000).

TNF-α and FasL are important mediators of inflammation, and they play a role in apoptosis. Studies performed in mouse models of ALS and patients with ALS show increases in TNF-α. In ALS patients, antigenic TNF-α and its soluble receptors measured by ELISA were significantly higher in ALS patients than in healthy controls (Poloni et al., 2000). RT-PCR showed increased TNF-α mRNA expression in spinal cords of G93A mice at 4 months of age, correlating with the onset of astroglial activation (Elliott, 2001). Levels of TNF-α message increased as the mice matured and became weaker, reaching a maximum at 7.5–8 months of age in low copy number G93A mice (Elliott, 2001). The mRNA for TNF-α receptors was also present. A study using RPAs showed increased Fas-associated death domain (FADD) and TNF-α receptor p55 at 80 d, which increased further at 120 d in high-expressing G93A mice (Hensley et al., 2002). Using *in situ* hybridization, TNF-α was increased in the lumbar spinal cord of G37R SOD1 mice at 7 and 10 months of age, and the signal was unchanged in the absence of IL-1β (Nguyen et al., 2001). Gene expression profiling using a Clontech (Mountain View, CA) array showed increased TNF-α expression at 11 weeks of age (5.3-fold) in G93A SOD1 mice, which increased further at 14 and 17 weeks (8-fold) (Yoshihara et al., 2002).

Glial cells are the major source of TNF-α expression in the CNS. We found that both lumbar spinal cord motor neurons and glia from G93A SOD1 mice express high levels of TNF-α, and this occurs at 60 d, well before the onset of symptoms. The increased immunoreactivity was much more pronounced at 90 and 110 d of age. An increase in TNF-α mRNA was confirmed by real-time RT-PCR in G93A mice at 110 d. Double labeling of TNF-α with GFAP confirmed expression of TNF-α in astrocytes (Fig. 1). This is consistent with a previous study in which TNF-α immunoreactivity was increased at 17 weeks of age in microglia and motor neurons of G93A SOD1 mice (Yoshihara et al., 2002).

Fas triggers cell death in embryonic motoneurons by a pathway requiring upregulation of neuronal nitric oxide synthase and involving Daxx, apoptosis signal-regulated kinase 1, and p38 as well as the FADD/caspase-8 pathway (Raoul et al., 2002). This pathway was not found in other cells. It was upregulated in motoneurons from transgenic mice with the G37R, G85R, or G93A mutations. This is of interest, because TNF-α upregulates FasL (Pinkoski et al., 2002) and enhances FasL-induced cell death *in vivo* (Ghezzi et al., 1998). FasL immunostaining increased in the lumbar spinal cord of G93A mice as early as 40 d of age. FasL immunostaing in neurons is apparent because of their size and morphology; we used double labeling to show that astrocytes stained for FasL, and this colocalized with GFAP (Fig. 2). Increased FasL immunostaining was observed in human postmortem spinal cord tissues, and TNF-α immunostaining was found in the neurons of adjacent sections, suggesting that FasL and TNF-α are coexpressed in these neurons (Fig. 3).

Because both TNF-α and FasL immunostaining were increased in G93A mice, we examined the effects of thalidomide and its analog lenalidomide, which inhibits the stability of TNF-α mRNA (Moreira et al., 1993). These inhibitors significantly inhibited TNF-α and FasL expression in motor neurons of G93A

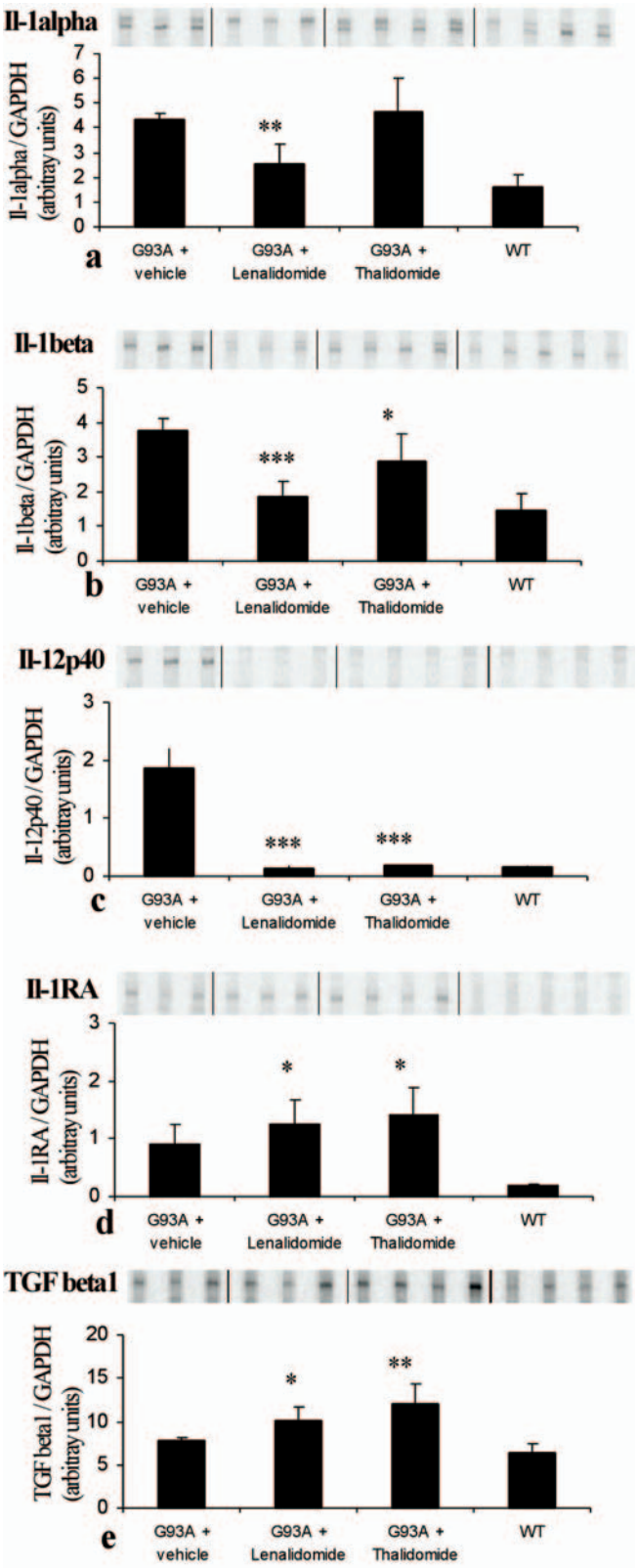

mice. There was a delay of disease onset and a significant attenuation of disease progression in G93A SOD1 mice (Figs. 4–6). The survival data in this study suggest that these compounds may have efficacy if treatment is started from the onset of symptoms, because there was a slowing in progression of disease (see curve slope in Fig. 5) with both of these compounds as well as a delay in the onset of disease.

Quantitative RT-PCR showed that both thalidomide and lenalidomide significantly reduced TNF-α mRNA levels at 110 d of age. Both compounds also inhibited IL-12p40, IL-1α, and IL-1β. IL-1RA and TGF-β1 mRNA were upregulated in G93A mice treated with thalidomide and lenalidomide (Fig. 8).

Our findings provide additional evidence for a role of pro-inflammatory cytokines in ALS and suggest that TNF-α and FasL and related cytokines have important triggering roles in the pathogenesis of ALS in initiating a cell death pathway(s). TNF-α binds to TNF receptor-1 and activates it to ligate with TNF-α receptor-associated death domain (TRADD), forming the DISC that leads to activation of caspase-8, resulting in Bid cleavage and the activation of executioner caspases-3, -6, and -7. FasL works in a similar way by binding to Fas/CD95 receptor and activate it to cause FADD ligation and DISC formation, which also leads on to caspase-8 activation, Bid cleavage, and, ultimately, activation of caspases-3, -6, and -7 (Nagata, 1997, 1999; Pinkoski et al., 2000; Ugolini et al., 2003). Because these two pathways converge on caspase-8 activation, they may have synergistic effects. Our study provides the first evidence that thalidomide and lenalidomide may have therapeutic value for treatment of human ALS.

In this study, the efficacy of lenalidomide was slightly superior to thalidomide. Lenalidomide inhibited TNF-α with less potency compared with thalidomide; in contrast, lenalidomide was more potent in inhibiting other cytokines such as IL-12p40, IL-1α, and IL-1β. This could be the underlying reason for higher potency of lenalidomide over thalidomide. However, our data suggest that these compounds are targeting other cytokines, and it also suggests that many pro-inflammatory cytokines may act together via one or several pathways to cause motor neuron degeneration in ALS. Furthermore, thalidomide and lenalidomide are able to upregulate anti-inflammatory cytokines such as IL-1RA and TGF-β1, which may have neuroprotective effects. These results suggest that maybe many pathways are blocked by thalidomide and lenalidomide and many are activated.

Thalidomide (Thalomid) is currently Food and Drug Administration (FDA) approved for the acute treatment of the cutaneous manifestations of moderate to severe erythema nodosum leprosum, and a new drug application for lenalidomide (Revlimid) has been submitted to the FDA for the treatment of patients with transfusion-dependent anemia attributable to low or intermediate-1 risk myelodysplastic syndromes associated with a deletion of 5q cytogenetic abnormality. In both erythema nodosum leprosum and myelodysplastic syndromes, upregulation of TNF-α production is postulated to contribute to disease pathogenesis. Because thalidomide is known to cause birth defects, we

←

Figure 8. Cytokine analysis and the effect of thalidomide and lenalidomide in G93A mice spinal cord total RNA. Spinal cord total RNA was used against a RPA multiprobe of cytokines. ***a***, IL-1α RNA was elevated in vehicle-treated G93A mice compared with wild type (N1020 controls) and significantly reduced in lenalidomide-treated G93A mice while unchanged in thalidomide-treated G93A mice. ***b***, IL-1β RNA was elevated in vehicle-treated G93A mice compared with wild type (N1020 controls) and significantly reduced by lenalidomide but not thalidomide treatment. ***c***, IL-12p40 RNA was elevated in vehicle-treated G93A mice compared with wild type (N1020 controls) and significantly reduced in both lenalidomide- and thalidomide-treated G93A mice. ***d***, IL-1RA RNA was elevated in vehicle-treated G93A mice compared with wild type (N1020 controls) and significantly elevated further in both lenalidomide- and thalidomide-treated G93A mice. ***e***, TGF-β1 RNA was not changed significantly in vehicle-treated G93A mice compared with wild type (N1020 controls) but significantly elevated further in both lenalidomide- and thalidomide-treated G93A mice. Cytokine RNA amounts in different samples were normalized against (L32 + GAPDH) RNA multiplied by 1000 and presented as an arbitrary number per (L32 + GAPDH) RNA (*$p < 0.5$; **$p < 0.05$; ***$p < 0.005$; Student's t test). WT, Wild type. Values are mean ± SEM.

emphatically warn that thalidomide should be prescribed under strict guideline if a clinical trial is to be conducted.

The suppression of spinal cord TNF-α mRNA in our study by thalidomide and lenalidomide, hence extension of survival in G93A mice, suggests that this class of immunomodulatory agents may have efficacy in diseases of the CNS associated with inflammatory neuronal damage. Thalidomide and lenalidomide therefore have promise as therapeutic agents for the treatment of ALS.

References

Almer G, Vukosavic S, Romero N, Przedborski S (1999) Inducible nitric oxide synthase up-regulation in a transgenic mouse model of familial amyotrophic lateral sclerosis. J Neurochem 72:2415–2425.

Almer G, Guegan C, Teismann P, Naini A, Rosoklija G, Hays AP, Chen C, Przedborski S (2001) Increased expression of the pro-inflammatory enzyme cyclooxygenase-2 in amyotrophic lateral sclerosis. Ann Neurol 49:176–185.

Bartlett JB, Dredge K, Dalgleish AG (2004) The evolution of thalidomide and its IMiD derivatives as anticancer agents. Nat Rev Cancer 4:314–322.

Boireau A, Bordier F, Dubedat P, Peny C, Imperato A (1997) Thalidomide reduces MPTP-induced decrease in striatal dopamine levels in mice. Neurosci Lett 234:123–126.

Bruijn LI, Becher MW, Lee MK, Anderson KL, Jenkins NA, Copeland NG, Sisodia SS, Rothstein JD, Borchelt DR, Price DL, Cleveland DW (1997) ALS-linked SOD1 mutant G85R mediates damage to astrocytes and promotes rapidly progressive disease with SOD1-containing inclusions. Neuron 18:327–338.

Consilvio C, Vincent AM, Feldman EL (2004) Neuroinflammation, COX-2, and ALS—a dual role? Exp Neurol 187:1–10.

Corral LG, Haslett PA, Muller GW, Chen R, Wong LM, Ocampo CJ, Patterson RT, Stirling DI, Kaplan G (1999) Differential cytokine modulation and T cell activation by two distinct classes of thalidomide analogues that are potent inhibitors of TNF-α. J Immunol 163:380–386.

Elliott JL (2001) Cytokine upregulation in a murine model of familial amyotrophic lateral sclerosis. Brain Res Mol Brain Res 95:172–178.

Ghezzi P, Mennini T (2001) Tumor necrosis factor and motoneuronal degeneration: an open problem. Neuroimmunomodulation 9:178–182.

Ghezzi P, Bernardini R, Giuffrida R, Bellomo M, Manzoni C, Comoletti D, Di Santo E, Benigni F, Mennini T (1998) Tumor necrosis factor is increased in the spinal cord of an animal model of motor neuron degeneration. Eur Cytokine Netw 9:139–144.

Gurney ME, Pu H, Chiu AY, Dal Canto MC, Polchow CY, Alexander DD, Caliendo J, Hentati A, Kwon YW, Deng HX, Chen W, Zhai P, Sufit RL, Siddique T (1994) Motor neuron degeneration in mice that express a human Cu,Zn superoxide dismutase mutation. Science 264:1772–1775.

Hall ED, Oostveen JA, Gurney ME (1998) Relationship of microglial and astrocytic activation to disease onset and progression in a transgenic model of familial ALS. Glia 23:249–256.

Hensley K, Floyd RA, Gordon B, Mou S, Pye QN, Stewart C, West M, Williamson K (2002) Temporal patterns of cytokine and apoptosis-related gene expression in spinal cords of the G93A-SOD1 mouse model of amyotrophic lateral sclerosis. J Neurochem 82:365–374.

Hensley LL, Ranganathan G, Wagner EM, Wells BD, Daniel JC, Vu D, Semenkovich CF, Zechner R, Kern PA (2003) Transgenic mice expressing lipoprotein lipase in adipose tissue. Absence of the proximal 3′-untranslated region causes translational upregulation. J Biol Chem 278:32702–32709.

Hirano A (1996) Neuropathology of ALS: an overview. Neurology 47:S63–S66.

Kiaei M, Kipiani K, Chen J, Calingasan NY, Beal MF (2005a) Peroxisome proliferator-activated receptor-gamma agonist extends survival in transgenic mouse model of amyotrophic lateral sclerosis. Exp Neurol 191:331–336.

Kiaei M, Kipiani K, Petri S, Choi DK, Chen J, Calingasan NY, Beal MF (2005b) Integrative role of cPLA with COX-2 and the effect of non-steriodal anti-inflammatory drugs in a transgenic mouse model of amyotrophic lateral sclerosis. J Neurochem 93:403–411.

Kiaei M, Kipiani K, Chen J, Calingasan NY, Beal MF (2006) Celastrol blocks motor neuron cell death and extends life in transgenic mouse model of amyotrophic lateral sclerosis. Neurodegenerative Dis, in press.

Kriz J, Nguyen MD, Julien JP (2002) Minocycline slows disease progression in a mouse model of amyotrophic lateral sclerosis. Neurobiol Dis 10:268–278.

Leigh PN, Ray-Chaudhuri K (1994) Motor neuron disease. J Neurol Neurosurg Psychiatry 57:886–896.

Li M, Ona VO, Guegan C, Chen M, Jackson-Lewis V, Andrews LJ, Olszewski AJ, Stieg PE, Lee JP, Przedborski S, Friedlander RM (2000) Functional role of caspase-1 and caspase-3 in an ALS transgenic mouse model. Science 288:335–339.

Moreira, A. L. Sampaio, E. P. Zmuidzinas, A. Frindt, P. Smith, K. A. Kaplan G (1993) Thalidomide exerts its inhibitory action on tumor necrosis factor α by enhancing mRNA degradation. J Exp Med 177:1675–1680.

Munoz-Fernandez MA, Fresno M (1998) The role of tumour necrosis factor, interleukin 6, interferon-gamma and inducible nitric oxide synthase in the development and pathology of the nervous system. Prog Neurobiol 56:307–340.

Nagata S (1997) Apoptosis by death factor. Cell 88:355–365.

Nagata S (1999) Fas ligand-induced apoptosis. Annu Rev Genet 33:29–55.

Nguyen MD, Julien JP, Rivest S (2001) Induction of proinflammatory molecules in mice with amyotrophic lateral sclerosis: no requirement for proapoptotic interleukin-1β in neurodegeneration. Ann Neurol 50:630–639.

Pinkoski MJ, Brunner T, Green DR, Lin T (2000) Fas and Fas ligand in gut and liver. Am J Physiol Gastrointest Liver Physiol 278:G354–G366.

Pinkoski MJ, Droin NM, Green DR (2002) Tumor necrosis factor α upregulates non-lymphoid Fas-ligand following superantigen-induced peripheral lymphocyte activation. J Biol Chem 277:42380–42385.

Poloni M, Facchetti D, Mai R, Micheli A, Agnoletti L, Francolini G, Mora G, Camana C, Mazzini L, Bachetti T (2000) Circulating levels of tumour necrosis factor-α and its soluble receptors are increased in the blood of patients with amyotrophic lateral sclerosis. Neurosci Lett 287:211–214.

Raoul C, Estevez AG, Nishimune H, Cleveland DW, deLapeyriere O, Henderson CE, Haase G, Pettmann B (2002) Motoneuron death triggered by a specific pathway downstream of Fas. potentiation by ALS-linked SOD1 mutations. Neuron 35:1067–1083.

Ripps ME, Huntley GW, Hof PR, Morrison JH, Gordon JW (1995) Transgenic mice expressing an altered murine superoxide dismutase gene provide an animal model of amyotrophic lateral sclerosis. Proc Natl Acad Sci USA 92:689–693.

Robertson J, Beaulieu JM, Doroudchi MM, Durham HD, Julien JP, Mushynski WE (2001) Apoptotic death of neurons exhibiting peripherin aggregates is mediated by the proinflammatory cytokine tumor necrosis factor-α. J Cell Biol 155:217–226.

Rosen DR, Siddique T, Patterson D, Figlewicz DA, Sapp P, Hentati A, Donaldson D, Goto J, O'Regan JP, Deng HX, et al (1993) Mutations in Cu/Zn superoxide dismutase gene are associated with familial amyotrophic lateral sclerosis. Nature 362:59–62.

Schiffer D, Cordera S, Cavalla P, Migheli A (1996) Reactive astrogliosis of the spinal cord in amyotrophic lateral sclerosis. J Neurol Sci [Suppl] 139:27–33.

Siddique T, Nijhawan D, Hentati A (1996) Molecular genetic basis of familial ALS. Neurology 47:S27–S34.

Tartaglia LA, Goeddel DV (1992) Two TNF receptors. Immunol Today 13:151–153.

Tewari M, Dixit VM (1996) Recent advances in tumor necrosis factor and CD40 signaling. Curr Opin Genet Dev 6:39–44.

Ugolini G, Raoul C, Ferri A, Haenggeli C, Yamamoto Y, Salaun D, Henderson CE, Kato AC, Pettmann B, Hueber AO (2003) Fas/tumor necrosis factor receptor death signaling is required for axotomy-induced death of motoneurons *in vivo*. J Neurosci 23:8526–8531.

Venters HD, Dantzer R, Kelley KW (2000) A new concept in neurodegeneration: TNF-α is a silencer of survival signals. Trends Neurosci 23:175–180.

West MJ, Slomianka L, Gundersen HJ (1991) Unbiased stereological estimation of the total number of neurons in thesubdivisions of the rat hippocampus using the optical fractionator. Anat Rec 231:482–497.

Wong PC, Pardo CA, Borchelt DR, Lee MK, Copeland NG, Jenkins NA, Sisodia SS, Cleveland DW, Price DL (1995) An adverse property of a familial ALS-linked SOD1 mutation causes motor neuron disease characterized by vacuolar degeneration of mitochondria. Neuron 14:1105–1116.

Yoshihara T, Ishigaki S, Yamamoto M, Liang Y, Niwa J, Takeuchi H, Doyu M, Sobue G (2002) Differential expression of inflammation- and apoptosis-related genes in spinal cords of a mutant SOD1 transgenic mouse model of familial amyotrophic lateral sclerosis. J Neurochem 80:158–167.